Multiple Plane Phase Retrieval Algorithm Based On Inverse Regularized Imaging

Artem Migukin
Department of Signal Processing, Tampere University of Technology
P.O. Box 553, 33101 Tampere, Finland
artem.migukin@tut.fi

April 29, 2010

Abstract

We reconstruct a spatially distributed wave field from a number of observations, obtained in different sensor planes, parallel to the object plane. The proposed wave field reconstruction procedure can be treated as a multiple plane iterative Gerchberg-Saxton algorithm [1]. We estimate a complex-valued object distribution using module observations from the sensor planes. Because of finite size of sensors the diffraction transform which defines the wave field propagation can be ill-posed, and the regularization is an important component of the inverse. The algorithm is studied by numerical experiments performed for amplitude and phase object distributions. It is shown that the proposed method allows reconstructing the whole wave fields using various wave field propagation models for different setup parameters. It is shown that the usage of the prior information about the type of the object distribution yield to the clear advantage in the reconstruction accuracy of the proposed parallel algorithm comparing with the successive iterative method [2].

1 Introduction

The reconstruction of the whole wave field (both amplitude and phase) is an important problem utilized in different technical and scientific applications, e.g. for $3D$ imaging or nondestructive testing. The phase of radiation scattered from an object carries important information about an object surface and its properties. The phase can not be measured directly, thus we recover the phase from a number of intensity measurements. There are two groups of the wave field reconstruction methods: interferometric one with a reference beam and methods without a reference beam (phase retrieval). The phase retrieval techniques are much more reliable and technically simpler than the interferometric ones, in particular, because of the simplicity of the optical setup. Furthermore, the phase retrieval approach is more robust with respect to various disturbances (e.g. vibrations).

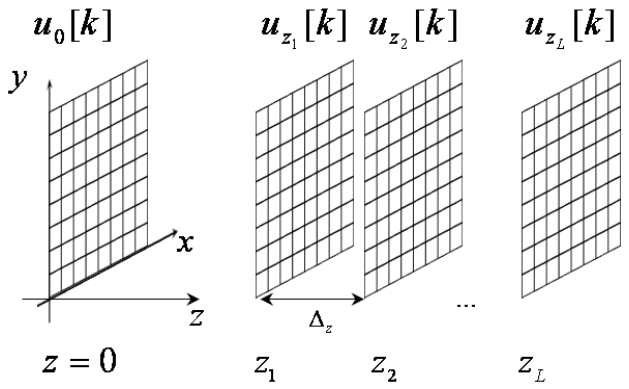

Figure 1: Multiple plane wave field reconstruction scenario: $u_0[k]$ and $u_{z_l}[k]$ are discrete complex amplitudes in the object and measurement planes respectively, $l = 1, ..., L$.

Mathematically and computationally the phase retrieval from the module measurements is not a trivial problem. In this paper we study a novel technique based on the parallel usage of the observations from all sensor planes simultaneously for the reconstruction of the $2D$ wave field in the object plane and $3D$ wave field distributions in the observation planes. The planar laser beam scattered by an object propagates through the space. The intensity of the resulting wave field distribution is registered by digital sensors in the sensor planes parallel to the object plane (see Fig.1).

The Gerchberg-Saxton-Fienup iterative algorithm ([1], [3]) is the most popular phase recovery method, based on the essential usage of a prior knowledge on the object size and object type (phase or amplitude modulation of the wave field). The idea is that the phases missing in observations are recovered iteratively applying the magnitude constraints in object and sensor planes. This technique has been studied, modified and developed in a flow of publications (see [4]) and the further generalizations of this technique have resulted in various modifications for different application areas. For instance, in [5] a multi-plane modification of the algorithm is developed in order to obtain a desired wave field distributions in different planes.

In this work we consider the wave field distribution in the object plane as the only unknown of the problem which one-to-one defines the wave fields for sensor planes. In this approach prior information on the object such as the size and modulation type is used in order to improve the accuracy of the wave field reconstruction. The main contribution of this paper concerns the developments of the whole wave field phase retrieval algorithm for different wave field propagation methods (e.g. the discrete diffraction transform (DDT) [6], [7], or the conventional angular spectrum decomposition, ASD) and numerical comparative analysis of the proposed parallel phase retrieval algorithm versus the successive method presented in [2]. The influence of the prior information in the object plane on the wave field reconstruction accuracy is analyzed. We consider the reconstruction of the object wave fields with

amplitude (AM) or phase (PM) modulations. It is shown that the spatially adaptive regularization used in the inverse imaging results in the further improvement of the algorithm performance.

2 Wave field propagation model

Let $u_0(x)$ and $u_{z_l}(x)$, $x \in \mathbb{R}^2$, $l = 1, ..., L$, denote the complex-valued wave field distributions in the object and sensor planes, respectively. $z_l = z_1 + (l-1) \cdot \Delta_z$ indicates a distance between the parallel object and $l-th$ sensor planes, Δ_z is a distance between two sensor planes, z_1 is a distance from the object to the first measurement plane and L is a number of the observation planes (sensor positions). We assume that the wave field distributions in the object and sensor planes are pixel-wise invariant. This assumption is natural for all sort of digital sensors and used as a pixel-wise approximation for the object plane. Because of this pixelation we obtain the sampled version of the continuous wave field distributions: $u_0(x) \rightarrow u_0[k]$, $u_{z_l}(x) \rightarrow u_{z_l}[k]$, where $k = (k_x, k_y) \in \mathbb{Z}^2$ is a two dimensional vector with integer components. In Fig.1 this multi-plane phase retrieval model is presented.

For the pixel-wise object distribution and the discrete sensor the link between $u_0[k] = |u_0[k]| \cdot \exp(j \cdot \phi_0[k])$ and $u_{z_l}[k] = |u_{z_l}[k]| \cdot \exp(j \cdot \phi_{z_l}[k])$ is given in the frequency domain as

$$U_{z_l}[f] = A_{z_l,z_o}[f] \cdot U_o[f], \tag{1}$$

where $f = (f_x, f_y) \in \mathbb{Z}^2$ is the spatial frequency, $U_{z_l}[f]$ and $U_o[f]$ are calculated as the $2D$ Fourier transform of $u_o[k]$ and $u_{z_l}[k]$ using $\mathcal{FFT}$.

The ASD discrete transfer function is given analytically as [8]:

$$A_{z_l,z_o}[f] = \exp(j2\pi \frac{z_l}{\lambda} \cdot \sqrt{1 - \frac{\lambda^2}{N_l^2 \cdot \Delta^2} ||f||_2^2}), \tag{2}$$

where $||f||_2^2 < (N_l^2 \cdot \Delta^2)/(\lambda^2)$, λ is the wavelength, Δ is the pixel size (we assume that the pixels are square $\Delta \times \Delta$) and $N_l \times N_l$ is the size (in pixels) of the wave field distribution in the $l-th$ observation plane.

In DDT (rather in $F-DDT$, [6]) the calculation is performed for extended double size versions of $u_o[k]$ and $u_{z_l}[k]$ zero padded to the double size of the images. The frequency domain operation is produced in $F-DDT$ for the double size images in order to the DDT forward propagation be accurate. This sort of double size calculations are typical for accurate convolutional techniques (e.g. [9]).

3 Phase retrieval algorithm

Let us assume for a moment that the complex-valued u_{z_l} are known. Then the reconstruction of u_o can be produced in the frequency domain according to the following optimization formulation

$$\hat{U}_o[f] = \arg\min_{U_o[f]} J, J = ||\sum_{l=1}^{L} U_{z_l}[f] - A_{z_l,z_o}[f] \cdot U_o[f]||_2^2 + \alpha^2 ||U_o[f]||_2^2, \tag{3}$$

Here $||U_o[f]||_2^2 = \sum_f |U_o[f]|^2$ and α^2 is a regularization parameter. The routine calculations give the estimate of $U_o[f]$ in the form

$$\hat{U}_o[f] = \frac{1}{\sum_{l=1}^{L} |A_{z_l,z_o}[f]|^2 + \alpha^2} \sum_{l=1}^{L} A^*_{z_l,z_o}[f] U_{z_l}[f], \tag{4}$$

where '$*$' stands for the complex-conjugate variable. The criterion in (3) corresponds to the standard Tikhonov's quadratic regularization of the ill-posed inverse problems [10]. We use the formula (4) in order to derive the algorithm for the case when only magnitude/module data are available instead of the complex-valued one.

Let the observations in the sensor planes be given as

$$o_{z_l}[k] = |u_{z_l}[k]| + \varepsilon_l[k], \tag{5}$$

where $\varepsilon_l[k] \sim \mathcal{N}(0, \sigma^2)$ are measurement noises. Substitute these noisy observations in (3) instead of $u_{z_l}[k]$, then we arrive at the following iterative algorithm, which allows reconstructing both the object and observation wave fields:

$$\hat{u}_0^{(t)}[k] = \sum_{l=1}^{L} \mathcal{FFT}^{-1}\{\frac{A^*_{z_l,z_o}[f] \cdot \mathcal{FFT}\{v_l^{(t-1)}[k]\}}{\sum_{l=1}^{L} |A_{z_l,z_o}[f]|^2 + \alpha^2}\} \tag{6}$$

$$\hat{u}_{z_l}^{(t)}[k] = \mathcal{FFT}^{-1}\{A_{z_l,z_o}[f] \cdot \mathcal{FFT}\{\hat{u}_0^{(t)}[k]\}\}, \tag{7}$$

$$\hat{\phi}_{z_l}^{(t)}[k] = angle(\hat{u}_{z_l}^{(t)}[k]),\ q_l^{(t)}[k] = (o_{z_l}[k] \cdot I_l[k] + |\hat{u}_{z_l}^{(t)}[k]| \cdot (1 - I_l[k])), \tag{8}$$

$$v_l^{(t)}[k] = q_l^{(t)}[k] \cdot \exp(j \cdot \hat{\phi}_{z_l}^{(t)}[k]),\ t = 1, 2... \tag{9}$$

The expressions (6)-(9) define the *iterative multiple plane parallel algorithm*, which can be treated as a generalization of the Gerchberg-Saxton algorithm. The equation (6) of this algorithm define the object wave field estimate, obtained from estimates in the sensor planes (backward propagation). The complex-valued $\hat{u}_o^{(t)}[k]$ can be corrected according to a prior information about the object distribution. The estimates in the sensor planes are exploited in parallel for the calculation of the object estimate. The estimate in the object plane is used for prediction (forward propagation) in the sensor planes (see, Eq. (7)). The modules of these predictions are corrected (Eq. (9)) by the given observations.

In particular, for $F - DDT$ with double size extended images and kernels the formula $o_{z_l}[k] \cdot I_l[k] + |u_{z_l}[k]| \cdot (1 - I_l[k])$ replaces the extended version of the magnitude $u_{z_l}[k]$ by the observations (5) in the middle part of the double size image and preserves the magnitudes $u_{z_l}[k]$ calculated for the outside of this middle part. Here $I_l[k]$ is the indicator of the image area in the l-th observation plane, i.e. $I_l[k] = 1$ for the image area and equal to 0 otherwise. In this case we name this phase retrieval algorithm **M**ultiple Plane **F**requency **DDT** ($MF - DDT$). For the single size calculations $I_l[k]$ is always equal to 1 for all l.

The object estimate for the ASD frequency domain models becomes simpler because $|A_{z_l,z_o}[f]|^2 = 1$, $A^*_{z_l,z_o}[f] = A_{-z_l,z_o}[f]$, thus we do not need regularization. The object estimate can be found in the form

$$\hat{u}_0^{(t)}[k] = \frac{1}{L}\sum_{l=1}^{L}\mathcal{FFT}^{-1}\{ASD^*_{z_l,z_o}[f]\cdot\mathcal{FFT}\{v_l^{(t-1)}[k]\}\} \quad (10)$$

In the single-beam multiple-intensity phase reconstruction ($SBMIR$) algorithm [2] the phase reconstruction is produced by the wave field propagation modeling from one sensor plane to the next following one with a circle loop going from the last sensor plane to the first one. The study of this algorithm demonstrates the efficiency of this technique in simulations and for real experimental data [11]. The proposed technique (6)-(9) is essentially different from $SBMIR$ by its structure because the observations from all planes are processed in parallel while in $SBMIR$ a plane-to-plane phase reconstruction is used. The use of the object distribution as the only estimated variable enables the parallel algorithm to involve prior information on the type of the object distribution (the amplitude or phase distribution of $u_o[k]$) as well as the object size. This additional information has a significant influence on the reconstruction accuracy. Numerical experiments confirm the advantage of this parallel processing, when the prior information (that the object is of the amplitude or phase type) is used in the algorithm. We assume that the size of the reconstructed object is known.

Moreover, a further development of the proposed approach is produced by using a varying spatially adaptive regularization instead of the simple Tikhonov‘s one. It is shown in [12] that this sort of regularization can be implemented as spatially adaptive filtering. In the developed modification of the proposed phase retrieval algorithm the phase and the magnitude of each iterative estimate $\hat{u}_o^{(t)}[k]$ are subjects of special filtering. For this filtering we use the powerful adaptive BM3D algorithm [13]. Simulations demonstrate an essential improvement in the object wave field reconstruction.

4 Numerical experiments

The numerical experiments are performed for amplitude and phase object distributions with the test-image *lena*. The images are square $N \times N$, $N = 256$ with the square pixels $\Delta \times \Delta$ of the same size in the object and sensor planes, $\Delta = 6.7\mu m$, the wavelength $\lambda = 632.8\ nm$. The "in-focus" distance is calculated as $z_f = N\Delta^2/\lambda = 18.16\ mm$ (see [7]). It is assumed that the additive noise in (5) is zero-mean Gaussian with $\sigma = 0.01$. The number of measurement planes varies: $L = [1, 20]$. The results are shown for 100 iterations of the algorithm. The distance between the measurement planes is fixed: $\Delta_z = 0.5mm$. The influence of the quantization of the observations on the wave field reconstruction accuracy is out of the scope in this work, and we assume that a high precision data from a sensor is given. The wave field reconstruction accuracy is given via the root mean square error ($RMSE$).

In Fig. 2 we present the reconstruction of the data obtained with the DDT assuming that this forward wave field propagation model yields to accurate results because it is precise and aliasing free for pixelated wave field distributions in the

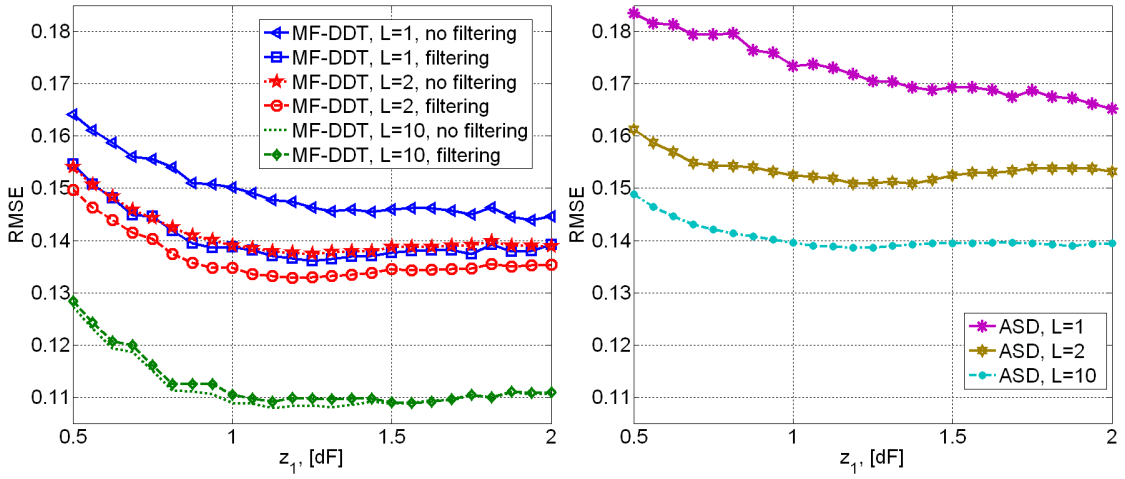

Figure 2: The accuracy (RMSE) of the object phase reconstruction by the $MF-DDT$ and ASD algorithms.

sensor and object. The accuracy of the phase reconstructions in the object plane is shown for different distances z_1. The accuracy of $MF-DDT$ is always better than that for the ASD algorithm (obtained according to (10)) with the relative improvement in $RMSE$ values about $30\% \div 50\%$. The adaptive regularization embedded in the $MF-DDT$ algorithm ($BM3D$ filtering) further improves the reconstruction quality. It is shown that there is an essential improvement generally for small L (say, $L=1,2$).

For the fair comparison of the proposed parallel algorithm with the original $SBMIR$ the following experiments are made with the observation data obtained using the ASD method.

Imaging of the reconstructed amplitude $|\hat{u}_0|$ and phase $\hat{\phi}_0$ distributions in the object plane is shown in Fig.3. These images correspond to the amplitude (AM) and phase modulation (PM) of the object distribution. We demonstrate the influence of the knowledge about the object type apriori on the quality of imaging. Here we show the reconstruction for the amplitude (Fig.3 (a)) and phase (Fig.3 (b)) object distributions provided that it is known in advance the corresponding object modulation. If the type of the distribution is unknown, a complex-valued object distribution is estimated. We show the amplitude and phase estimates for the AM in Fig.3 (c) and (d), and for PM in Fig.3 (e) and (f) respectively.

In Fig.4 we compare the object wave field reconstruction accuracy (for AM), obtained by the proposed algorithm (6)-(9) and by the successive $SBMIR$. The original successive iterative process of $SBMIR$ has no direct connection to the object plane, and it is not able to use the prior information on its distribution (see "$SBMIR, \text{complex}$"). We have modified this algorithm and included the object plane in this successive recursive procedure. The corresponding result is shown as "$SBMIR, abs$". The curves in Fig.4 show that the proposed algorithm gives a better accuracy for the amplitude object, when the type of the object distribution is used for the estimation ("ASD, abs"). If we do not use the prior information on the

Figure 3: The object wave field reconstruction, $L = 10$, $z_1 = 1.5 \cdot z_f$: (a) $|\hat{u}_0|$, AM, $RMSE = 0.01$, (b) $\hat{\phi}_0$, PM, $RMSE = 0.1$, (c) $|\hat{u}_0|$, AM, $RMSE = 0.04$, (d) $\hat{\phi}_0$, AM, $RMSE = 0.192$, (e) $|\hat{u}_0|$, PM, $RMSE = 0.14$, (f) $\hat{\phi}_0$, PM, $RMSE = 0.172$.

object distribution and estimate the object distribution as a complex-valued one, the $SBMIR$ algorithm gives a better accuracy than the proposed algorithm. In this case the result for the parallel algorithm is marked as "$ASD, \text{complex}$". The $SBMIR$ algorithm converges very quickly and the increase of the number of iterations does not yield to a significant improvement in accuracy. The accuracy value for the proposed method increases monotonically, but slower than for $SBMIR$. For large number of iterations and L the proposed algorithm demonstrates better accuracy.

The reconstruction accuracy of the wave field distributions in all measurement planes is considered for the phase and amplitude separately. It is found that a larger number of the observation planes L results in monotonically better accuracy for both the object and sensor planes. This improvement is valuable for small L (say, $L = 2, 3$) and not essential for larger L. The reconstruction quality increase rapidly for $L < 10$ both for PM and AM, with a significant improvement achieved for $L < 7$ (for example, if we take $L = 5$ instead of $L = 2$ the accuracy in $RMSE$ values will increase by approximately 50% or more). For larger L (we increase the number of planes from $L = 10$ to $L = 20$) this improvement is much smaller: by approximately 30% for the object wave field and by less than 25% for the mean value of $RMSE$ for the module or phase reconstruction over all measurement planes. Note, that the results for different observation planes are quite close with the standard deviation from the mean values not more than 6%. For larger σ (say, $\sigma = 0.05$) the improvement of wave field reconstruction for larger L is also not so significant for larger L (a slope of the $RMSE$ curves decreases).

In the reconstruction of the whole complex-valued object wave field the concordance of the phase estimates $\hat{\phi}_{z_l}[k]$ (see Eq. (8)) is of very importance, because the phase component of the final object estimate (the sum in (6)) should have close

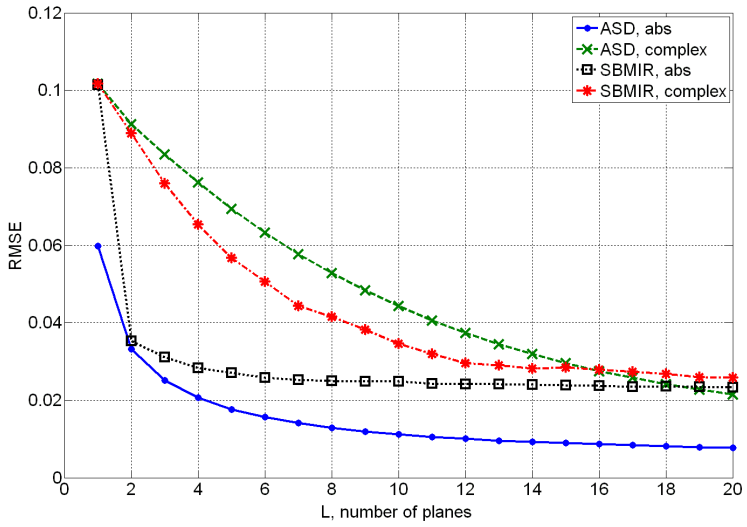

Figure 4: The $RMSE$ reconstruction accuracy of the object magnitude versus the number of planes L, AM, $z_1 = 1.5 \cdot z_f$: the proposed parallel algorithm versus $SBMIR$.

values. The wrapping effect could lead to a quite strong damage for the parallel algorithm, poor quality of reconstruction and imaging of the final estimates. In Fig.3 (d) an example of this wrapping effect for AM can be seen. The phase wrapping effects in the reconstructed phase distributions are seen as bright white sports. Note that it also results in the worse reconstruction of the object amplitude.

5 Conclusions

In this work we present a phase retrieval algorithm based on simultaneous processing of the data (with ASD and DDT as the forward propagation model) from a number of parallel observation planes. Numerical experiments demonstrate the applicability of the proposed algorithm for the reconstruction of the whole complex-valued wave field distributions. The improvement of the reconstruction accuracy depending on the increase of the number of observation planes is shown. The prior information on the object type allows the proposed algorithm to obtain better accuracy with respect to the successive $SBMIR$ algorithm.

References

[1] R. W. Gerchberg and W. O. Saxton, "A practical algorithm for the determination of phase from image and diffraction plane pictures," *Optik* 35, pp. 227–246, 1972.

[2] G. Pedrini, W. Osten, and Y. Zhang, "Wave-front reconstruction from a sequence of interferograms recorded at different planes," *Opt. Lett.,* 30, pp. 833-835, 2005.

[3] J. R. Fienup, "Reconstruction of an object from the modulus of its Fourier transform," *Opt. Lett.* 3, pp. 27–29, 1978.

[4] R. Piestun and J. Shamir, "Synthesis of 3D light fields and applications," *Proc. of the IEEE*, vol. 90, pp. 222-244, 2002.

[5] G. Sinclair, et al., "Interactive application in holographic optical tweezers of a multi-plane Gerchberg-Saxton algorithm for three-dimensional light shaping," *Opt. Express,* vol.12, pp. 1665-1670, 2004.

[6] V. Katkovnik, J. Astola, and K. Egiazarian, "Discrete diffraction transform for propagation, reconstruction, and design of wavefield distributions," *Appl. Opt.* 47, pp. 3481-3493, 2008.

[7] V. Katkovnik, A. Migukin, and J. Astola, "Backward discrete wave field propagation modeling as an inverse problem: toward perfect reconstruction of wave field distributions," *Appl. Opt.* 48, pp. 3407-3423, 2009.

[8] J. W. Goodman, Introduction to Fourier Optics, New York: McGraw-Hill Inc, Second Edition, 1996.

[9] F. Shen and A. Wang, "Fast-Fourier-transform based numerical integration method for the Rayleigh–Sommerfeld diffraction formula," *Appl. Opt.* 45, pp. 1102-1110, 2006.

[10] A.N. Tikhonov and V.Y. Arsenin. Solution of ill-posed problems, New York: Wiley, 1977.

[11] P. Almoro, G. Pedrini and W. Osten, "Complete wavefront reconstruction using sequential intensity measurements of a volume speckle field," *Appl. Opt.*, Vol. 45 Issue 34, pp. 8596-8605, 2006.

[12] K. Dabov, A. Foi, and K. Egiazarian, "Image restoration by sparse 3D transform-domain collaborative filtering," *Proc. SPIE Electronic Imaging '08*, no. 6812-07, San Jose, California, USA, 2008

[13] K. Dabov, A. Foi, V. Katkovnik, and K. Egiazarian, "Image denoising with block-matching and 3D filtering," *Proc. SPIE Electronic Imaging* '06, no. 6064A-30, San Jose, California, USA, 2006.